

Disorder induced quantized conductance with fractional value and universal conductance fluctuation in three-dimensional topological insulators

Lei Zhang¹, Jianing Zhuang¹, Yanxia Xing^{1,2} and Jian Wang^{1,*}

¹*Department of Physics and the Center of Theoretical and Computational Physics, The University of Hong Kong, Hong Kong, China*

²*Department of Physics, Beijing Institute of Technology, Beijing 100081, China*

We report a theoretical investigation on the conductance and its fluctuation of three-dimensional topological insulators (3D TI) in Bi_2Se_3 and Sb_2Te_3 in the presence of disorders. Extensive numerical simulations are carried out. We find that in the diffusive regime the conductance is quantized with fractional value. Importantly, the conductance fluctuation is also quantized with a universal value. For 3D TI connected by two terminals, three independent conductances G_{zz} , G_{xx} and G_{zx} are identified where z is the normal direction of quintuple layer of 3D TI (see inset of Fig.1). The quantized conductance are found to be $\langle G_{zz} \rangle = 1$, $\langle G_{xx} \rangle = 4/3$ and $\langle G_{zx} \rangle = 6/5$ with corresponding quantized conductance fluctuation 0.54, 0.47, and 0.50. The quantization of average conductance and its fluctuation can be understood by theory of mode mixing. The experimental realization that can observe the quantization of average conductance is discussed.

PACS numbers: 72.10.Fk, 73.20.Fz, 73.25.+i,

Recently, the topological insulator (TI), a new state of matter, has attracted a lot of theoretical and experimental attention.¹⁻³ The TI has an insulating energy gap in the bulk states which behaves like the general insulator, but it has exotic gapless metallic states on its edges or surfaces. The TI is first predicted in two-dimensional (2D) systems, e.g., the graphene and HgTe/CdTe quantum well. It has been generalized⁴ in 3D and confirmed experimentally.⁵ The 2D TI has the gapless helical edge states and exhibits the quantum spin Hall effect while in 3D TI the conducting state is helical surface state. This helical edge or surface states are topologically protected and are robust against all time-reversal-invariant impurities. Many interesting physical phenomena have been predicted including Majorana fermion⁶, topological magnetoelectric effect⁷, magneto-optical Kerr and Faraday effects.⁸ There are also many studies on disordered TI. It was found by Li et al that in the presence of disorder,⁹ a new phase called topological Anderson insulator can be induced. The complete physical picture and mechanism of topological Anderson insulator (TAI) was given by Groth et al¹⁰ using an effective medium theory. Recently, the TAI was also predicted in 3D TI.¹¹ Both analytic and numerical results show that disorder can induce strong topological Anderson insulator in 3D.

Disorder can affect mesoscopic systems in an important way. For instance, it is well known that, in the diffusive regime, the conductance fluctuation of the mesoscopic system assumes a universal value that is independent of system parameters and depends only on dimensionality and symmetry of the system.¹² For a 2D TI (HgTe/CdTe quantum well), it was found that the spin-Hall conductance fluctuation is universal.¹³ It will be of great interest to explore the universal behavior of conductance and its fluctuation in 3D TI.

In this paper, we have studied the effect of disorder on topological surface states in 3D TI for Bi_2Se_3 system using extensive numerical simulation. Due to anisotropy

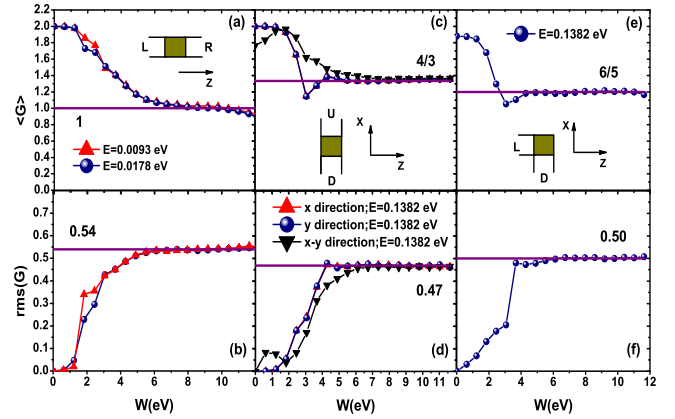


FIG. 1: (Color online) Conductance and its fluctuation vs disorder strength for different transport directions, G_{zz} for panel (a) and (b), G_{xx} , G_{yy} and G_{xy} for panel (c) and (d), G_{zx} for panel (e) and (f). Each data point on the figure is averaged over 5000 configurations.

of the Bi_2Se_3 system, there are three independent two-terminal conductance G_{zz} , G_{xx} and G_{zx} where z is the normal direction of quintuple layer of 3D TI. We found that in the diffusive regime, the average conductance is quantized with fractional value 1, 4/3, 6/5, respectively, for G_{zz} , G_{xx} and G_{zx} (in units of e^2/h). The corresponding conductance fluctuation is also quantized. By varying the disorder strength W and the Fermi energy E_F inside the bulk gap, the phase diagrams of conductance and its fluctuation in the plane of (W, E_F) were constructed, showing the same quantized conductance and fluctuation for a wide range of E_F and W . By introducing the number of effective transmission and reflection channels, the quantized conductance as well as the quantized fluctuation can be understood by the mode mixing theory.¹⁴ The quantized values of conductance and fluctuation from the proposed effective mode mixing theory

are in excellent agreement with our numerical results. It is known that as disorder increases the electron transport goes through the ballistic and the diffusive regime and finally enters the localized regime. Our numerical result shows that the evolution of topological surface states in the presence of disorders undergoes three stages: (1). the topological surface states are protected up to a critical disorder strength beyond which the topological surface states are destroyed while the bulk gap is present. At this stage, the conducting channels are non-topological surface states. This is true when the system begin entering the diffusive regime. (2). While still in the diffusive regime but at large disorders, the bulk gap is destroyed and the conducting channels are bulk states. (3). For large enough disorders, the system becomes localized and there is no conducting channel available. Furthermore, four-terminal conductance and its fluctuation were calculated. Similar quantization behaviors for conductance and fluctuation were found.

In our numerical simulation, we discretize spatial coordinates of the continuous effective \mathbf{k} space Hamiltonian H_{TI} in Ref.15 on the square lattice:

$$H_{TI} = \sum_{\mathbf{i}} \Psi_{\mathbf{i}}^{\dagger} H_{\mathbf{ii}} \Psi_{\mathbf{i}} + \sum_{\vec{\alpha}=(\vec{\delta}_x, \vec{\delta}_y, \vec{\delta}_z), \mathbf{i}} \Psi_{\mathbf{i}}^{\dagger} H_{\mathbf{i}, \vec{\alpha}} \Psi_{\mathbf{i}+\vec{\alpha}} + H.c. (1)$$

where $\mathbf{i} = (ix, iy, iz)$ is the site index and $\vec{\delta}_x, \vec{\delta}_y, \vec{\delta}_z$ are unit vectors along x, y and z directions where z is the normal direction of quintuple layer of 3D TI. $\Psi_{\mathbf{i}} = (a_{\mathbf{i}}, b_{\mathbf{i}}, c_{\mathbf{i}}, d_{\mathbf{i}})^T$, and $a_{\mathbf{i}}, b_{\mathbf{i}}, c_{\mathbf{i}}, d_{\mathbf{i}}$ represents the four annihilation operators of electron on the site \mathbf{i} with the state indices $|P1_z^+, \uparrow\rangle, |P2_z^-, \uparrow\rangle, |P1_z^+, \downarrow\rangle, |P2_z^-, \downarrow\rangle$. In Eq.(1), $H_{\mathbf{ii}}$ and $H_{\mathbf{i}, \vec{\delta}_x}$ are 4×4 Hamiltonian that are given by $H_{\mathbf{ii}} = (C + 2D_1/a^2 + 4D_2/a^2)I_{4 \times 4} + (M - 2B_1/a^2 - 4B_2/a^2)\Gamma_0$, $H_{\mathbf{i}, \vec{\delta}_x} = -D_2/a^2 I_{4 \times 4} + B_2/a^2 \Gamma_0 - iA_2/(2a)I_{4 \times 4}^a$, $H_{\mathbf{i}, \vec{\delta}_y} = -D_2/a^2 I_{4 \times 4} + B_2/a^2 \Gamma_0 - iA_2/(2a)\Gamma_1$, $H_{\mathbf{i}, \vec{\delta}_z} = -D_1/a^2 I_{4 \times 4} + B_1/a^2 \Gamma_0 - iA_1/(2a)\Gamma_2$, where $\Gamma_{0,1,2} \equiv (I_{2 \times 2} \otimes s_z, s_y \otimes I_{2 \times 2}, s_z \otimes I_{2 \times 2})$ and I^a is anti-diagonal identity matrix. Static Anderson type disorder is added to the on-site energy with a uniform distribution in the interval $[-W/2, W/2]$ where W characterizes the strength of the disorder. Here a is the lattice constant, and $A_1, A_2, B_1, B_2, C, D_1, D_2$ and M are system's parameters taken from Ref.15.

By using Green's functions, the charge conductance from the terminal- β to the terminal- α can be calculated by using Landauer-Büttiker formula $G_{\alpha\beta}(E) = (e^2/h)T_{\alpha\beta}$, and $T_{\alpha\beta} = \text{Tr}[\Gamma_{\alpha} G^r \Gamma_{\beta} G^a]$ is the transmission coefficient. The linewidth function $\Gamma_{\alpha}(E) = i[\Sigma_{\alpha}^r - \Sigma_{\alpha}^a]$ and the Green's functions $G^{r/a}(E)$ can be calculated from $G^r = [G^a]^{\dagger} = [EI - H_C - \sum_{\alpha} \Sigma_{\alpha}^r]^{-1}$, where H_C is Hamiltonian matrix of the central scattering region and I is the unit matrix with the same dimension as that of H_C , Σ_{α}^r are self energy of external leads and can be calculated numerically¹⁶. The conductance fluctuation is defined as $\text{rms}(G) \equiv \sqrt{\langle G^2 \rangle - \langle G \rangle^2}$, where $\langle \dots \rangle$ denotes averaging over an ensemble of samples with different disorder con-

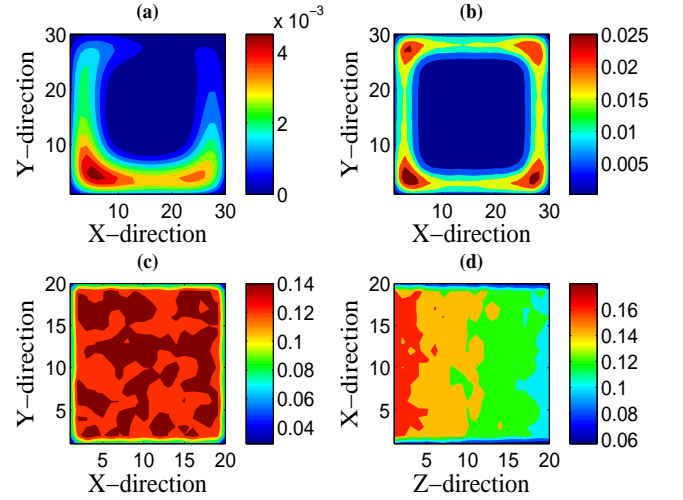


FIG. 2: (Color online) Averaged DOS in the middle slices of the central simulation box with injected wave from left lead with different disorder strength.

figurations of the same strength W . In the following the average conductance and its fluctuation are measured in unit of e^2/h .

In the numerical calculations, we choose the realistic material parameters for Bi_2Se_3 ¹⁵ and perform calculations on a $L \times L \times L$ cubic sample with $L = 20$ and the lattice constant $a = 5 \text{ \AA}$. Since each site has four orbitals, the dimension of the Hamiltonian or Green's function becomes 32000 for this system making the simulation very computational demanding. We first study the two terminal device by considering different transport directions in the presence of Anderson type disorder. As expected, our numerical simulation shows that transport properties along x direction is the same as that of y direction. So for the two-terminal structure there are four conductances: G_{zz}, G_{xx}, G_{xy} , and G_{zx} that are plotted in Fig.1 along with their fluctuations against the disorder strength. Here the Fermi energy is inside the bulk gap so that only topological surface states are conducting channels. In general, our results show that the topological surface states are gradually destroyed in the presence of small disorders. As the strength of disorder increases, the system enters the diffusive regime and the conductance becomes quantized for a wide range of disorder strength. Importantly, this quantization of conductance is accompanied by the quantized conductance fluctuation. This conductance fluctuation is universal since it is independent of parameters such as Fermi energy and disorder strength as shown in Fig.3. From Fig.1, we see that the quantized conductance takes fractional value with $\langle G_{zz} \rangle = 1$, $\langle G_{xx} \rangle = \langle G_{xy} \rangle = 4/3$, and $\langle G_{zx} \rangle = 6/5$. Two points worth mentioning from Fig.1(c) and (d): (1). Two set of curves for $\langle G \rangle$ and $\text{rms}(G)$ versus disorder strength along x direction and y direction are exactly the same which is expected. (2). For G_{xx} and G_{xy} , however, only their average conductance and its fluctuation in the

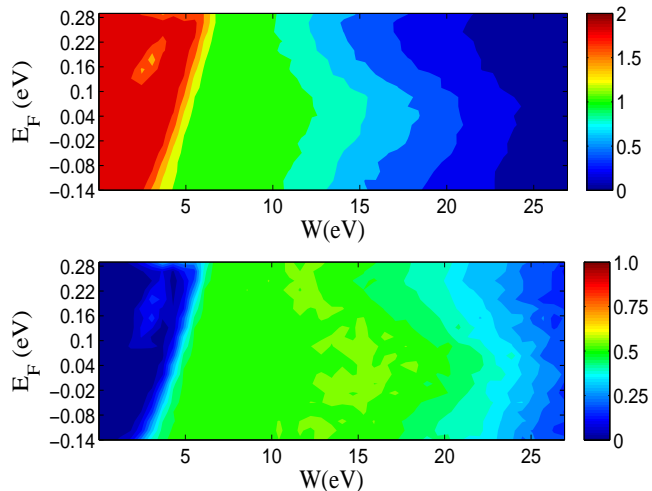


FIG. 3: (Color online) Phase diagram of conductance (panel (a)) and its fluctuation (panel (b)) in the plane of (W, E_F) . 1000 samples are collected in each point on the phase diagram calculation.

diffusive regime are the same. Its origin can be understood using the theory of mode mixing discussed below. To make sure that the quantization plateau lies in the diffusive regime, we have calculated the localization length ξ in the quantization plateau region for $W = [5, 10]$. Our results give $\xi/L = 6 \sim 8$ in this range of W indicating that the system is indeed in the diffusive regime.

The quantization of conductance in the diffusive regime can be described using the following phenomenological theory of mode mixing in the central region.¹⁴ For instance, for the transport along z direction, two incoming topological surface states are completely mixed in the scattering region in the diffusive regime with equal probability of going forward p_f and backward p_b , i.e., $p_f = p_b = 1/2$. Hence the conductance is $\langle G_{zz} \rangle = 2p_f = 1$. Alternatively, we can use the number of effective transmission channels ν_t and reflection channels ν_r with $\nu_t/\nu_r = p_f/p_b$. For G_{zz} , we have $\nu_r = \nu_f = 1$ so that $p_f = \nu_t/(\nu_t + \nu_r) = 1/2$. For G_{xx} , only partial mixing is achieved with $\nu_r = 1$ and $\nu_t = 2$, or $p_f = 2/3$. As a result, $\langle G_{xx} \rangle = 2p_f = 4/3$. Since x and y directions are equivalent, an incoming electron from x direction traversing in the scattering region find the same available ν_t along y direction as that of x direction. Hence $\langle G_{xx} \rangle = \langle G_{xy} \rangle$. To support this argument, we have calculated two-terminal conductance of a four-terminal device with four terminal on x - y plane (see the inset of Fig.4(b)). For an electron from L -lead, we should have $\langle G_{RL} \rangle = \langle G_{UL} \rangle = \langle G_{DL} \rangle$ if x and y directions are equivalent. This is indeed what we found numerically. In addition, the conductance fluctuations are also the same. For G_{zx} , $\nu_r = 1$ and $\nu_t = 3/2$ due to the partial mixing, or $\langle G_{zx} \rangle = 2p_f = 6/5$. In terms of the number of effective channels, the quantized conductance can be given by the following expression,

$$\langle G \rangle = 2 \frac{\nu_t \nu_r}{\nu_t + \nu_r}. \quad (2)$$

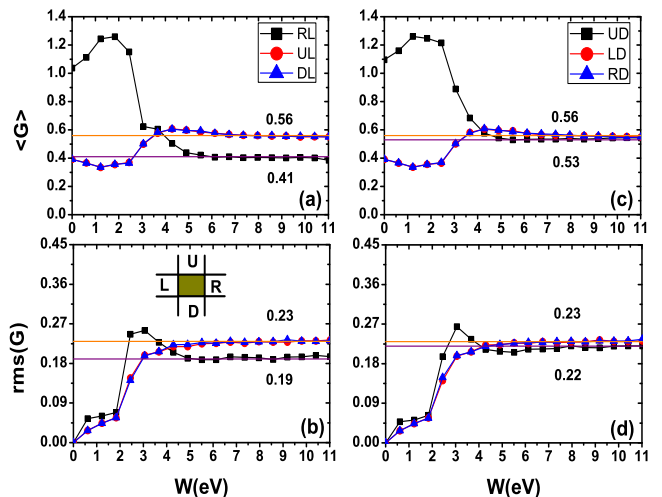


FIG. 4: (Color online) Conductance and its fluctuation vs disorder strength for different transport direction in four terminal cross-setup.

This ansatz gives the average conductance that agrees with our numerical result for the quantized conductance of two-terminal structures. The universal conductance fluctuations (UCF) can also be expressed in terms of the number of effective transmission and reflection channels,¹⁷

$$\text{rms}(G) = 4 \sqrt{\frac{\nu_t^2 \nu_r^2}{(\nu_t + \nu_r)^2 [4(\nu_t + \nu_r)^2 - 2]}}. \quad (3)$$

With $(\nu_r, \nu_f) = (1, 1)$, $(1, 2)$, and $(1, 1.5)$ for G_{zz} , G_{xx} , and G_{zx} , respectively, we find from Eq.(3) that $\text{rms}(G_{zz}) = 2/\sqrt{14} = 0.535$, $\text{rms}(G_{xx}) = 8/3/\sqrt{34} = 0.457$, and $\text{rms}(G_{zx}) = 12/5/\sqrt{23} = 0.500$ that are very close to our numerical results (see Fig.1).

We now examine the evolution of wave function as disorder strength is varied in the diffusive regime when the propagation is along z direction. In our numerical simulation we set $E_F = 0.1348\text{eV}$ in Fig.2(a),(b) and $E_F = 0.0178\text{eV}$ in Fig.2(c),(d). In the clean sample there are two pairs of topological surface states localized on the surface and separated in space so that the backscattering is forbidden. In Fig.2(a), we have shown the DOS of one of the topological surface states propagating along positive z direction. As the disorder is increased, these localized surface states become extended on the surface and the topological surface states are destroyed. However, current carrying states are still surface states and there is no DOS in the bulk (see Fig.2(b)). This behavior of bulk insulator persists when the average conductance becomes quantized in the diffusive regime, e.g., when $W = 6\text{eV}$ the system is a bulk insulator but the surface states is not topological protected. As disorder strength increases further the surface states gradually expand toward the center of the system and eventually become bulk states. At $W = 8\text{eV}$, the bulk gap is closed due to the disorders. In order to investigate the nature of mode mixing,

we calculate the DOS for electron coming from the left lead along z direction at $W = 8eV$. Fig.2(c) shows the average DOS in $x - y$ plane where 10000 configurations are collected. From Fig. 2, we see that two modes are fully mixed in $x - y$ plane due to the disorder scattering. In the $x - z$ plane (Fig.2(d)), the DOS is mainly distributed around the left region due to the suppression of transmission ($\langle G \rangle \simeq 1$).

To demonstrate the universal feature of the quantized conductance and its fluctuation, we have calculated the phase diagram where G_{zz} and $\text{rms}(G_{zz})$ are plotted in (W, E_F) plane (see Fig.3). In the calculation, the periodic condition in x direction is employed. The light green region shows the quantized conductance. For Fermi energy inside the energy gap in the clean sample, we see that the system goes quickly from topological insulator to the region of quantized conductance. As disorder strength increases, it slowly enters the localized regime. This phase diagram shows that the conductance and its fluctuation are independent of Fermi energy and disorder strength in a wide range.

Now we study the transmission coefficient $T_{\alpha\beta}$ of a four-terminal device shown schematically in the inset of Fig.4(b) where the leads L and R are along z direction and leads U and D are along x direction. In the calculation we have fixed $E_F = 0.0178eV$ and over 5000 samples are collected for each average. Fig.4 shows that in the diffusive regime, the conductance and its fluctuation are again quantized. When there are four terminals, however, the quantized conductance is no longer a fractional value. It is much smaller than that of the two-terminal case. This is not unexpected since there are two more terminals that electron can exit. To our surprise, the conductance fluctuation is also much smaller than that of the two-terminal case, nearly halved.

To provide further evidence of universal conductance fluctuation, we have performed calculation for another 3D TI in Sb_2Te_3 ¹⁸ on a $20 \times 20 \times 20$ cubic sample. Our numerical results give the same values of quantized conductance and fluctuation. So far, we have studied the influence of bulk disorder on the transport of 3D TI. We

have also calculated the averaged conductance and its fluctuation in the presence of "surface" disorder. Specifically, we have calculated G_{zz} when disorders are present only on the first layer or first three layers of surface of 3D TI in Bi_2Se_3 . The quantized conductance and its fluctuation again show the same quantized plateau as the case of the bulk disorder with the same quantized conductance and quantized fluctuation. Note that the conductance measurement with surface disorder has been carried out experimentally on Bi_2Se_3 .¹⁹⁻²¹ Since the quantization of conductance and fluctuation exist in a large window of disorder strength (corresponding to doping concentration in experiment), we believe that our results can be checked experimentally.

To summarize, we have carried out extensive numerical simulation to calculate the transport properties of disordered 3D TI. Our results show that in the diffusive regime, the two-probe conductance is quantized with fractional value $1, 4/3, 6/5$. The corresponding conductance fluctuation is also quantized. An effective mode mixing theory is proposed that gives quantized conductance and fluctuation in excellent agreement with our numerical results. The numerical results from different parameters including disorder strength and Fermi energy (from phase diagram of conductance and its fluctuation), types of disorders (bulk and surface disorder), and types of 3D TI (Bi_2Se_3 and Sb_2Te_3) suggest that the quantized conductance and quantized fluctuation is a universal property of 3D TI. We have also studied effect of disorder on topological surface states. We found that as disorder strength increases the conducting channels changes from topological surface states to non-topological surface states and finally to bulk states in the diffusive regime.

Acknowledgments This work was financially supported by Research Grant Council (HKU 705409P) and University Grant Council (Contract No. AoE/P-04/08) of the Government of HKSAR. This research is conducted using the HKU Computer Centre research computing facilities that are supported in part by the Hong Kong UGC Special Equipment Grant (SEG HKU09).

* Electronic address: jianwang@hku.hk

¹ J. E. Moore, Nature (London) 464, 194 (2010).

² M. Z. Hasan and C. L. Kane, Rev. Mod. Phys. 82, 3045 (2010).

³ X. L. Qi and S. C. Zhang, arXiv:1008.2026.

⁴ L. Fu and C.L. Kane, Phys. Rev. Lett. **100**, 096407 (2008); **102**, 216403 (2009).

⁵ D. Hsieh et al, Nature(London) **452**, 970 (2008).

⁶ L. Fu, and C. L. Kane, Phys. Rev. Lett. 100, 096407 (2008).

⁷ X.L. Qi, T.L. Hughes, and S.C. Zhang, Phys. Rev. B 78, 195424 (2008).

⁸ W.K. Tse and A.H. MacDonald, Phys. Rev. Lett. 105, 057401 (2010).

⁹ J. Li et al, Phys. Rev. Lett. **102**, 136806 (2009).

¹⁰ C.W. Groth et al, Phys. Rev. Lett. **103**, 196805 (2009).

¹¹ H.M Guo et al, Phys. Rev. Lett. **105**, 216601 (2010).

¹² L. B. Altshuler, JETP Lett. **41**, 648 (1985); P.A. Lee and A.D. Stone, Phys. Rev. Lett. **55**, 1622 (1985); P. A. Lee, A. D. Stone and H. Fukuyama, 1987 Phys. Rev. B **35**, 1039 (1987).

¹³ Z.H. Qiao et al, Phys. Rev. Lett. **101**, 016804 (2008).

¹⁴ D. A. Abanin and L. S. Levitov, Science **317**, 641 (2007).

¹⁵ H.J. Zhang et al, Science **5**, 438 (2009).

¹⁶ D. H. Lee and J. D. Joannopoulos, Phys. Rev. B **23**, 4997 (1981); M. P. Lopez Sancho et al., J. Phys. F **14**, 1205 (1984); **15**, 851 (1985).

¹⁷ Note that this expression is different from Eq.(4) in Ref.14.

¹⁸ Liu et al, Phys. Rev. B **82**, 045122 (2010).

¹⁹ J. Chen et al, Phys. Rev. Lett. **105**, 176602 (2010).

²⁰ H.T. He et al, Phys. Rev. Lett. **106**, 166805 (2011).

²¹ J. Wang et al, Phys. Rev. B **83**, 245438 (2011).